Prospective estimation of organ dose in CT under tube current modulation

Xiaoyu Tian[a)]
Department of Biomedical Engineering, Carl E. Ravin Advanced Imaging Laboratories, Department of Radiology, Duke University, Durham, North Carolina 27705

Xiang Li
Department of Physics, Cleveland State University, Cleveland, Ohio 44115

W. Paul Segars
Carl E. Ravin Advanced Imaging Laboratories, Department of Radiology, Medical Physics Graduate Program, Duke University Medical Center, Durham, North Carolina 27705

Donald P. Frush
Division of Pediatric Radiology, Department of Radiology, Medical Physics Graduate Program, Duke University Medical Center, Durham, North Carolina 27710

Ehsan Samei
Carl E. Ravin Advanced Imaging Laboratories, Department of Radiology, Medical Physics Graduate Program, Departments of Physics and Biomedical Engineering, Duke University Medical Center, Durham, North Carolina 27705

(Received 5 May 2014; revised 10 December 2014; accepted for publication 8 January 2015; published 17 March 2015)

Purpose: Computed tomography (CT) has been widely used worldwide as a tool for medical diagnosis and imaging. However, despite its significant clinical benefits, CT radiation dose at the population level has become a subject of public attention and concern. In this light, optimizing radiation dose has become a core responsibility for the CT community. As a fundamental step to manage and optimize dose, it may be beneficial to have accurate and prospective knowledge about the radiation dose for an individual patient. In this study, the authors developed a framework to prospectively estimate organ dose for chest and abdominopelvic CT exams under tube current modulation (TCM).

Methods: The organ dose is mainly dependent on two key factors: patient anatomy and irradiation field. A prediction process was developed to accurately model both factors. To model the anatomical diversity and complexity in the patient population, the authors used a previously developed library of computational phantoms with broad distributions of sizes, ages, and genders. A selected clinical patient, represented by a computational phantom in the study, was optimally matched with another computational phantom in the library to obtain a representation of the patient's anatomy. To model the irradiation field, a previously validated Monte Carlo program was used to model CT scanner systems. The tube current profiles were modeled using a ray-tracing program as previously reported that theoretically emulated the variability of modulation profiles from major CT machine manufacturers Li *et al.*, [Phys. Med. Biol. **59**, 4525–4548 (2014)]. The prediction of organ dose was achieved using the following process: (1) $CTDI_{vol}$-normalized-organ dose coefficients (h_{organ}) for fixed tube current were first estimated as the prediction basis for the computational phantoms; (2) each computation phantom, regarded as a clinical patient, was optimally matched with one computational phantom in the library; (3) to account for the effect of the TCM scheme, a weighted organ-specific $CTDI_{vol}$ [denoted as $(CTDI_{vol})_{organ,weighted}$] was computed for each organ based on the TCM profile and the anatomy of the "matched" phantom; (4) the organ dose was predicted by multiplying the weighted organ-specific $CTDI_{vol}$ with the organ dose coefficients (h_{organ}). To quantify the prediction accuracy, each predicted organ dose was compared with the corresponding organ dose simulated from the Monte Carlo program with the TCM profile explicitly modeled.

Results: The predicted organ dose showed good agreements with the simulated organ dose across all organs and modulation profiles. The average percentage error in organ dose estimation was generally within 20% across all organs and modulation profiles, except for organs located in the pelvic and shoulder regions. For an average $CTDI_{vol}$ of a CT exam of 10 mGy, the average error at full modulation strength ($\alpha = 1$) across all organs was 0.91 mGy for chest exams, and 0.82 mGy for abdominopelvic exams.

Conclusions: This study developed a quantitative model to predict organ dose for clinical chest and abdominopelvic scans. Such information may aid in the design of optimized CT protocols in

relation to a targeted level of image quality.
[http://dx.doi.org/10.1118/1.4907955]

Key words: CT, computed tomography, Monte Carlo, organ dose, patient-specific

1. INTRODUCTION

Computed tomography (CT) has become an indispensable imaging modality for the diagnosis of a broad range of diseases in both pediatric and adult populations.[1,2] Despite the significant clinical benefits provided by CT, concerns have been raised regarding the potential cancer risk induced by CT radiation exposure.[3] In this light, optimizing the radiation dose forms a core responsibility for the CT community.[4–6] As a fundamental step to manage and optimize radiation dose, it may be beneficial to quantify patient-specific radiation dose. Such dose estimates, particularly when known prospectively, could provide information useful for the design of individualized CT protocols, for the assessment and improvement of patient imaging management decisions, and for optimizing CT dose in relationship with image quality of the study.

In light of prospectively quantifying patient-specific radiation dose, previous studies have demonstrated it is feasible to use $CTDI_{vol}$-normalized-dose coefficients (h_{organ}) to predict organ dose based on the patient size and the $CTDI_{vol}$ value.[7–11] However, this methodology may not represent the widely used tube current modulation (TCM) scheme. Introduced more than a decade ago, tube current modulation technique has now been frequently implemented in clinical body CT exams. Quantifying the magnitude of organ dose under TCM, however, is practically challenging. The main challenge relates to the fact that the x-ray radiation is dynamically altered over the patient habitus for TCM examinations. To accurately estimate organ dose, one needs to model such change of irradiation condition and further integrate it with the anatomical feature of the patients. The prior studies have been able to use the concept of regional $CTDI_{vol}$ in conjunction with organ dose coefficients to assess organ dose.[1,12] However, the methodology has been applied to a limited number of human models, and is further oriented toward retrospective dose estimation for specific models.

The purpose of this study was to assess organ dose under TCM schemes using a prediction atlas-based approach. The prediction, applied to for chest and abdominopelvic exams, was achieved by combining a patient matching technique, a TCM scheme that emulates modulation profiles from major CT vendors, and Monte Carlo simulation results for a library of computational phantoms with representative sizes, ages, and genders. A validation study was further performed to quantify the accuracy of the proposed dose prediction technique.

2. MATERIALS AND METHODS

Organ dose is governed by two main factors: patient anatomy (patient size, organ location, and tissue composition) and x-ray irradiation field (including the effect of scanning x-ray tube voltage, bowtie filter, pitch, and tube current modulation). A prediction process was developed to effectively model both factors. To model the complexity and variety in patient anatomy, we used a previously developed library of computational phantoms covering a broad range of patient body habitus. A clinical patient, represented by a computational phantom in this study, was further optimally matched to one computational phantom in order to obtain a prior estimation of patient anatomy. As for the second factor, a previously validated Monte Carlo simulation program was used to simulate the scanner system and scanning trajectory during the exam. The detailed prediction process is outlined as follows:

2.A. Patient-specific computational models and matching technique

The library of computational models consisted of 58 adult patients (age range, 18–78 year old; weight range, 57–180 kg). The subjects reflected a wide coverage of ages and weight percentiles/BMI ranges so that a clinical patient could be well-represented by one or a group of computational phantoms (Fig. 1).

The formation of the library is detailed in early publications.[13,14] In summary, each XCAT phantom was created using a four-step process as detailed below. First, a patient's chest-abdominal-pelvis scan with arms above head was used as the basis for creating the phantom. Large organs within the CT image volume were segmented semimanually into 3D triangulated polygon models using Image Segment software (RAI Laboratories, Duke University, Durham, NC). Second, the segmented datasets were imported into a 3D fitting program (Rhinoceros, www.rhino3d.com) to build 3D nonuniform rational B-spline (NURBS) surfaces. Since the CT images only covered the chest, abdomen, and pelvis regions, we manually added the head, arms, and legs to the phantom using existing reference male and female XCAT models. The addition and morphing process needed for this step was performed with Rhinoceros modeling software. The scale factors for the head size and lengths of the legs and arms for each model were determined using the PeopleSize program based on the statistics of the US male and female population (http://www.openerg.com/psz/index.html). Third, a multichannel large deformation diffeomorphic metric mapping (MC-LDDMM) technique was used to obtain the outline of the computational model. As the last step, the phantom was examined by an experienced observer to ensure anatomical accuracy. The examination was performed by comparing the organ/structure volumes of the phantom to those predicted from ICRP Publication 89 based on the model height.[15] If necessary, minor adjustments were made by scaling undersized or oversized organs.

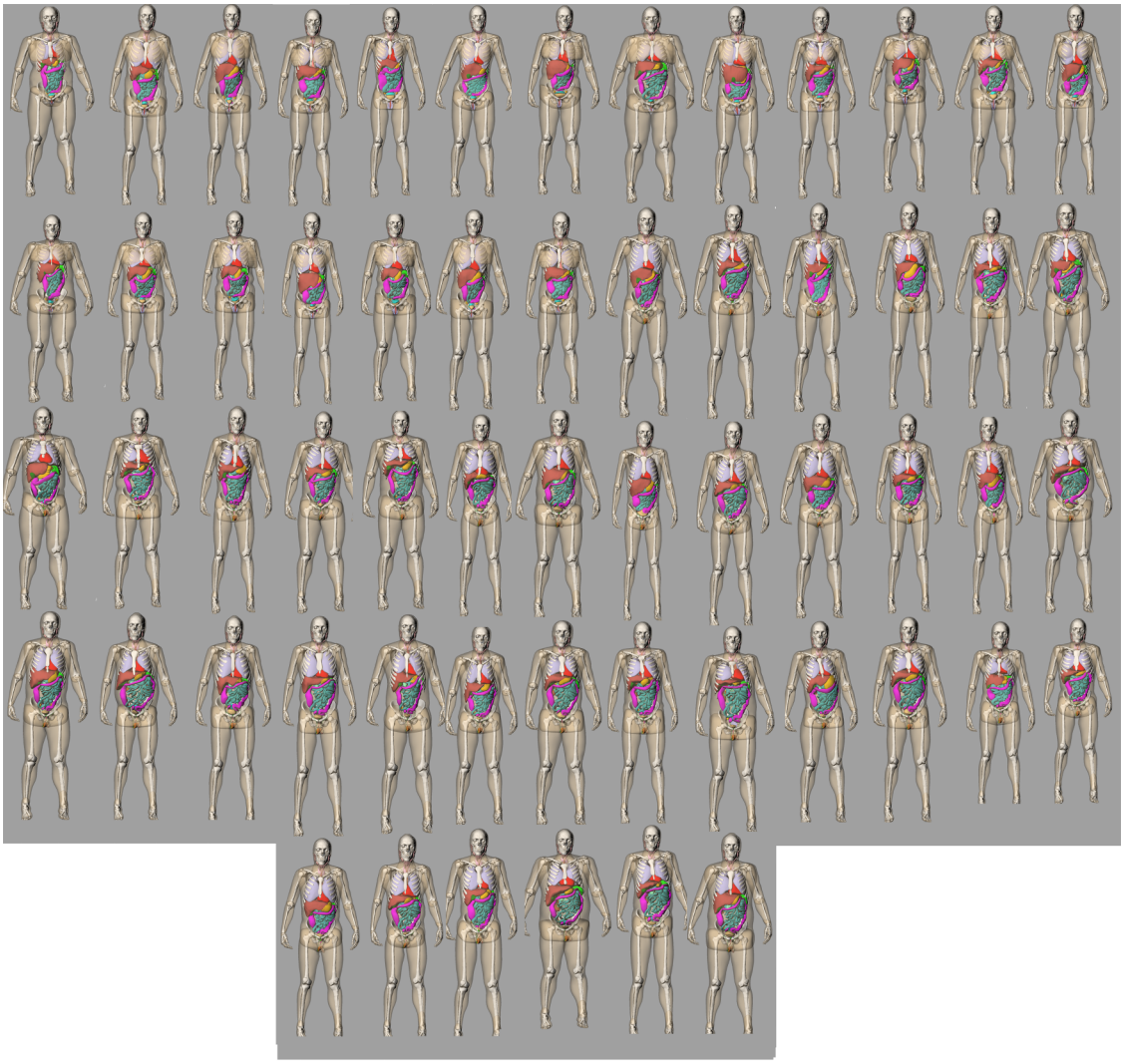

FIG. 1. 3D frontal views of the series of patient models used in this study.

The full-body patient models consisted of 43 and 44 organs for male and female patients, respectively, including most of the radiosensitive organs defined by ICRP publication 103.[16] All models were voxelized into a 3.45 mm resolution for input into the Monte Carlo simulation program.

With an atlas of computational phantoms that cover a broad range of human anatomy, a new clinical patient can be matched to a corresponding model that closely resembles the patient in terms of locations of major organs. In this study, each computational phantom was regarded as a clinical patient and matched to another phantom in the library (using a leave-one-out methodology). We used trunk height as an indicator for this matching. The trunk height is defined as the distance between the top of clavicle to the end of pelvic region. Figure 2 shows four pairs of matched models (male and female patients at 25% and 75% height and weight).

It should be noted that the matching process only ensures a close resemble of patient organ distribution in z dimension between the pairs. The overall body shape and size of the patient were accounted using the organ dose coefficients as detailed in Sec. 2.B. The trunk height was empirically found to be the best indicator for patient organ z dimensional distribution compared with BMI and patient weight.

2.B. CTDI-normalized-organ dose coefficients

As the prediction basis, Monte Carlo simulation was performed for each patient-specific model to estimated organ dose under fixed tube current. The simulation program was based on a benchmarked Monte Carlo subroutine package for photon, electron, and positron transport.[17,18] A commercial CT scanner was modeled (SOMATOM Definition Flash, Siemens Healthcare, Forcheim, Germany). The modeling of the system has been previously validated against physical measurements with discrepancies in dose estimates within −12% to +5%.[9] Clinical chest and abdominopelvic exams were simulated for each patient. For a chest scan, the image coverage was defined from 1 cm above the lung apex to 1 cm below the lung base. For an abdominopelvic scan, the image coverage was defined from 1 cm above the liver anterior to 1 cm below the ischium.

Organ doses were estimated by tallying the energy deposited in each organ. For the radiosensitive organs that were

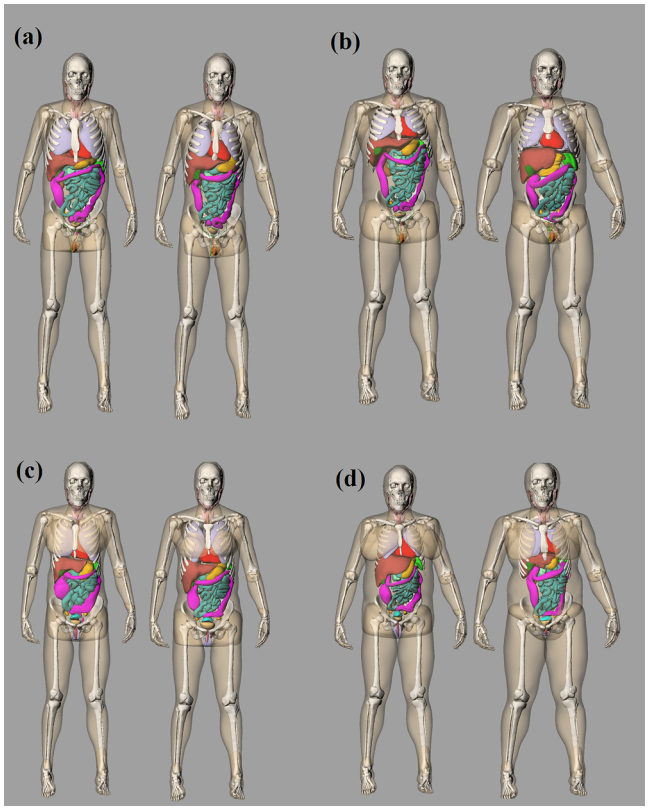

FIG. 2. Example patient-model matching pairs as determined by trunk height. (a) 25th percentile male, (b) 75th percentile male, (c) 25th percentile female, and (d) 75th percentile female.

not explicitly modeled [salivary glands, oral mucosa, and extrathoracic (ET) region], the dose values were approximated by using the dose values of neighboring organs (pharynx and larynx). $CTDI_{vol}$-normalized-organ dose coefficients were further determined for each organ, denoted as h_{organ}. The 32-cm-diameter CTDI phantom was used for all protocols.

The relationship between h_{organ} and average patient diameter was estimated as detailed in previous studies.[9–11] An exponential regression model was established as

$$h_{organ(chest)} = \exp(\alpha_o d_{chest} + \beta_o) \quad (1)$$

and

$$h_{organ(abdo)} = \exp(\alpha_o d_{abdo} + \beta_o), \quad (2)$$

where d_{chest} and d_{abdo} denote the average chest and abdominopelvic diameter, respectively.

2.C. Tube current modulation profile

The TCM profile can be either directly extracted from the CT scanner system or estimated based on its principle. In this study, we employed a ray-tracing algorithm to simulate the TCM profile. In a study by the IMPACT group,[19] the automatic exposure control systems of four CT manufacturers (GE, Siemens, Philips, and Toshiba) were evaluated using a cone-shaped phantom. The relationship between the tube current and phantom attenuation was evaluated. The study showed that for three of the manufacturers (GE, Siemens, and Toshiba), the tube current was exponentially related to phantom attenuation (ud). However, the strength of such a dependence was different across vendors, resulting in different behaviors of image quality across the patient population.

The logarithm of tube current (mA) can be modeled as a function of patient attenuation as

$$\ln(\mathrm{mA}) = \alpha^*(\mathrm{ud}) + \ln(\mathrm{mA}_o), \quad (3)$$

where the ud denotes the phantom attenuation, a denotes the modulation strength, which has a different value for different scanners, and mA_o corresponds to the fixed mA, nonmodulation mA DC level. The tube current modulation for some scanners aims to achieve constant noise levels across patient sizes and body regions (generally GE scanners). Thus, a would be equal to 1 to ensure constant noise in all measured CT projections and uniform noise across images. The tube current modulation for other scanners allows for higher noise in high-attenuating body regions and larger patients (generally Siemens scanners). The modulation strength can be adjusted to three levels (weak, average, and strong) to control how strong the mA is depending on patient attenuation. Thus, a can be varied in order to emulate this dependency.

In this work, a previously developed ray-tracing algorithm was used to model the mA modulation profile based on attenuation.[1] The algorithm estimated the attenuation at a given gantry angle, taking into account the geometry of the CT system, the fan angle of the x-ray beam, the polyenergetic x-ray energy spectrum, and the attenuation through the bowtie filter and the patient. A total of five mA modulation profiles were generated for each patient with a values of 0, 0.25, 0.5, 0.75, and 1 (Fig. 3). It should be noted that this study did not require the simulated mAs profile to precisely model the actual mAs profiles, which are usually proprietary and vary across vendors. Rather, the purpose was to generate a generalized and reasonable mA profile based on the principle of tube current modulation. An actual organ dose prediction scheme can either use a modeled mA profile or use an actual profile provided by the scanner.

2.D. Organ dose prediction

The atlas of computational phantoms and matching technique provide a prior estimation of patient anatomy, whereas the tube current modulation profile can be used to model the specific irradiation field. We further integrate the patient anatomical feature with the TCM in order to determine the radiation field encompassing the organ of interest. More specifically, a weighted organ-specific $CTDI_{vol}$ factor was computed as[1]

$$(\mathrm{CTDI_{vol}})_{organ,weighted} = \frac{\langle \mathrm{mA} \rangle_{organ,weighted}}{\langle \mathrm{mA} \rangle_{scan}} \mathrm{CTDI_{vol}} \quad (4)$$

and

$$\mathrm{mA}_{organ,weighted} = \frac{\sum_{z \in \{organ\}} \mathrm{mA}_z^* N_z}{\sum_{z \in \{organ\}} N_z}, \quad (5)$$

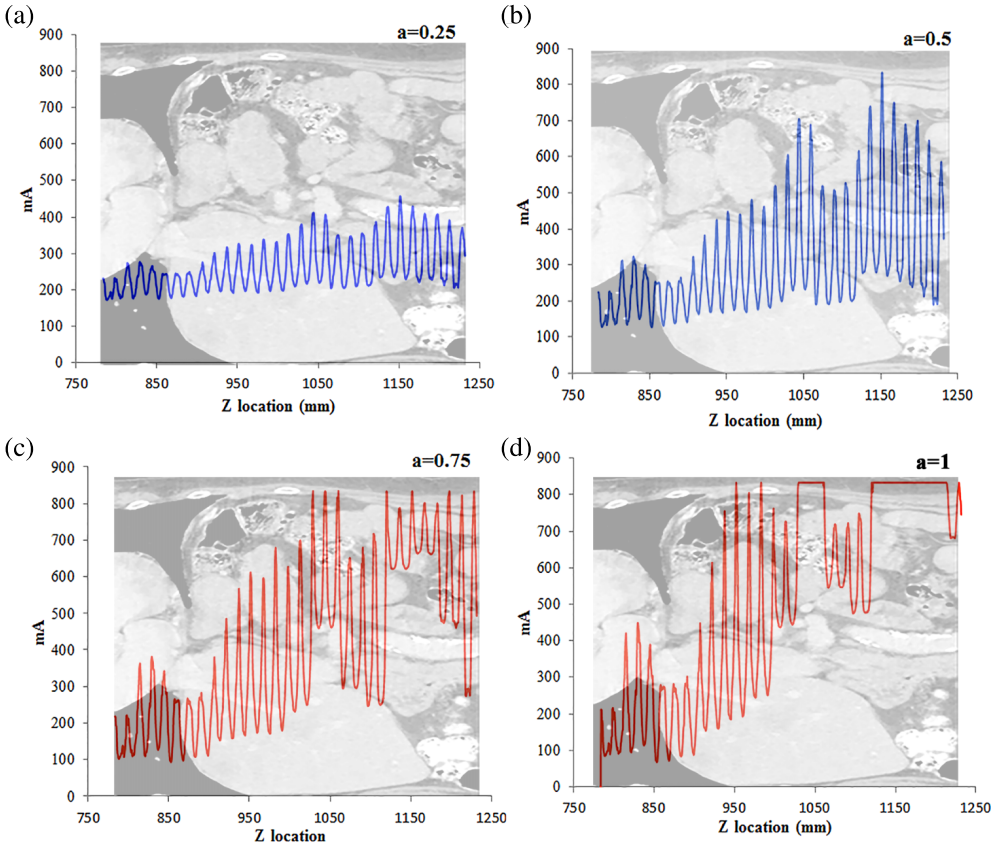

FIG. 3. Example tube current modulation profiles at four modulation strengths for a chest exam.

where $CTDI_{vol}$ refers to the $CTDI_{vol}$ reported on the CT scanner console, which was derived using the average mAs of the CT exam. mAz is the mAs value at location z, and N is the number of organ voxels in the axial slice at location z. Such organ-specific $CTDI_{vol}$ can be regarded as a regional $CTDI_{vol}$ that reflects the strength of radiation field for a specific organ. The organ dose under TCM was further predicted as

$$D_{TCM} = h_{organ}{}^{*}(CTDI_{vol})_{organ,weighted}, \quad (6)$$

where h_{organ} denotes the h factor estimated based on patient size as noted in Sec. 2.B, and D_{TCM} denotes the predicted organ dose for the patient under tube current modulation.

2.E. Validation of prediction accuracy of organ dose

The accuracy of the proposed prediction method was quantified using the following process: tube current modulation was incorporated into the Monte Carlo program; organ dose was estimated across the 58 patient models; each computational model, regarded as a clinical patient, was matched to one computational phantom in the library using the leave-one-out strategy. Organ dose was then predicted using the proposed method under five modulation strengths. Such a predicted organ dose was compared against the MC simulated organ dose values to quantify the prediction accuracy.

3. RESULTS

Figures 4 and 5 illustrate $CTDI_{vol}$-normalized-organ dose based on MC simulation (the gold standard) at five modulation strengths as a function of patient size across 58 computational models for chest and abdominopelvic scans, respectively. For the majority of organs within the scan coverage, organ dose coefficients show a gradual decrease with the increase of tube current modulation level. For chest scan, the average organ dose coefficients decreased 42.8% for the heart, and 25.0% for the lungs for scans with $a = 1$ as compared to no modulation ($a = 0$). For the abdominopelvic scan, the average organ dose coefficients decreased 33.8% for the stomach and 31.6% for the liver when implemented with full TCM modulation ($a = 1$) as compared to no modulation ($a = 0$). For a few organs located at specific regions (shoulder and pelvic), the organ dose coefficients increased when tube current is modulated. The thyroid dose coefficients under chest exam increased 73.4% as compared with fixed mA scans. Similarly, the testes dose coefficients under abdominopelvic scan increased 39.5% for full modulation condition as compared to no modulation ($a = 0$). Further, for constant tube current condition, organ dose coefficients show a strong exponential relationship with patient size. But with TCM, since the TCM profile is different for each patient, this exponential relationship is less definitive.

Comparing the results of Eq. (3) and full Monte Carlo simulation, Figs. 6 and 7 illustrate the prediction accuracy

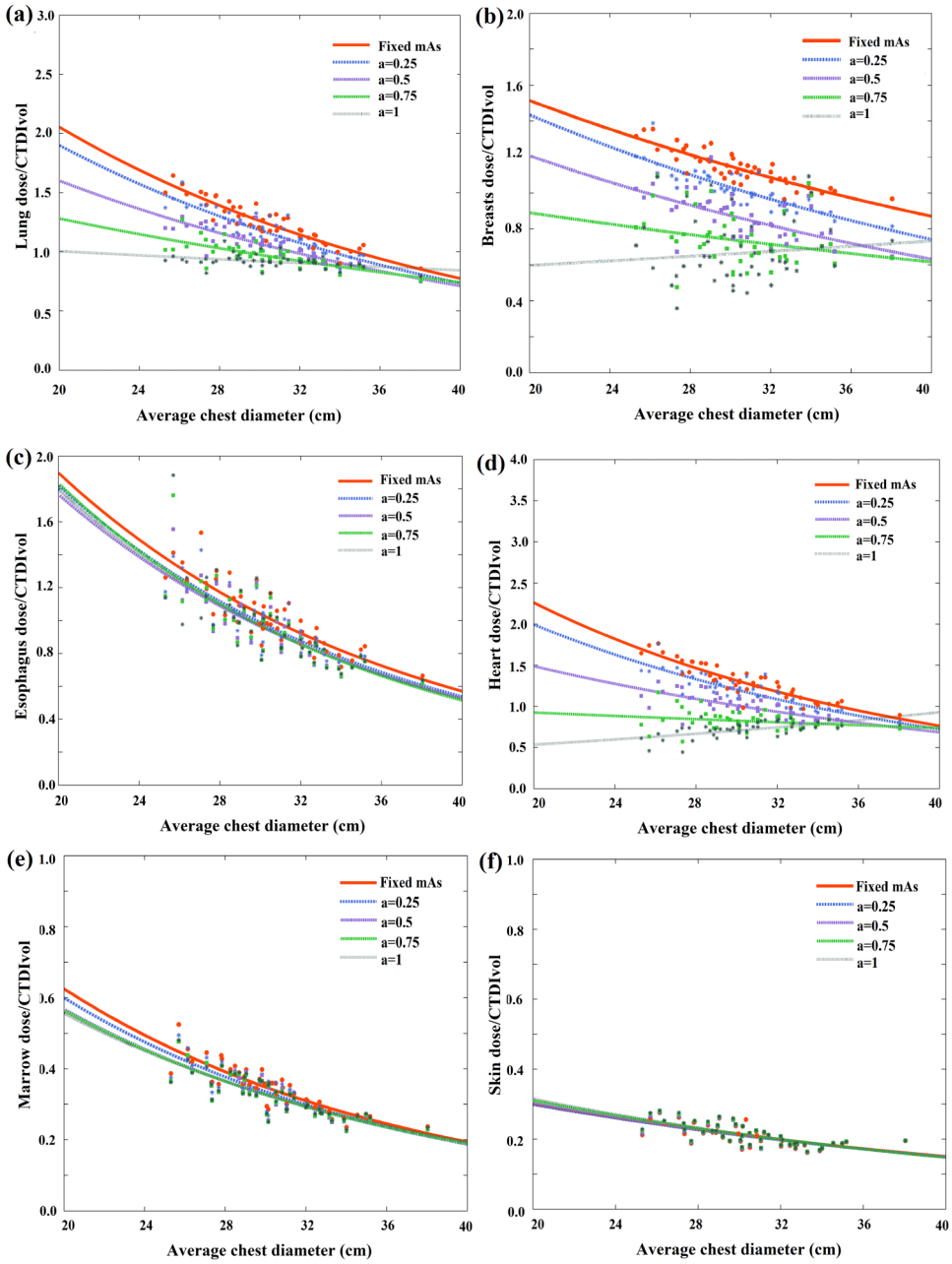

FIG. 4. Example $CTDI_{vol}$-normalized-organ dose coefficients for chest scans plotted against the average chest diameter at five modulation strengths. Among the five curves, the $CTDI_{vol}$-normalized-organ dose at fixed mA condition ($a = 0$) was used as the prediction basis. The other four curves were used as the gold standard for the prediction.

of organ dose at five tube current modulated strengths for chest and abdominopelvic scans, respectively. The histograms of prediction errors for six organs were plotted for each exam. The errors were further normalized by $CTDI_{vol}$ so that the accuracy of a given CT exam can be estimated. Given the average $CTDI_{vol}$ of a CT exam to be 10 mGy, the average error across all organs at full modulation ($a = 1$) was 0.91 mGy for chest exams and 0.82 mGy for abdominopelvic exams.

As tabulated in Tables I and II, the average percentage error in organ dose estimation was generally within 20% across all organs and modulation profiles, except for organs located in the pelvic and shoulder regions. For organs within the image coverage, the prediction error generally increased with the increasing level of tube current modulation. This can be explained by the fact that this prediction technique approximates the organ dose under TCM scan using the organ dose coefficients estimated from fixed mAs. Such approximation may produce less accurate results when the tube is changing rapidly within the axial dimension. Furthermore, the error is larger and more varied for organs within the scan range. This is because the organ mismatch error, which refers to the location difference of an organ in the patient compared to the corresponding matched computational model, is more influential for these organs compared with distributed organs and organs outside the scan range. For organs within the

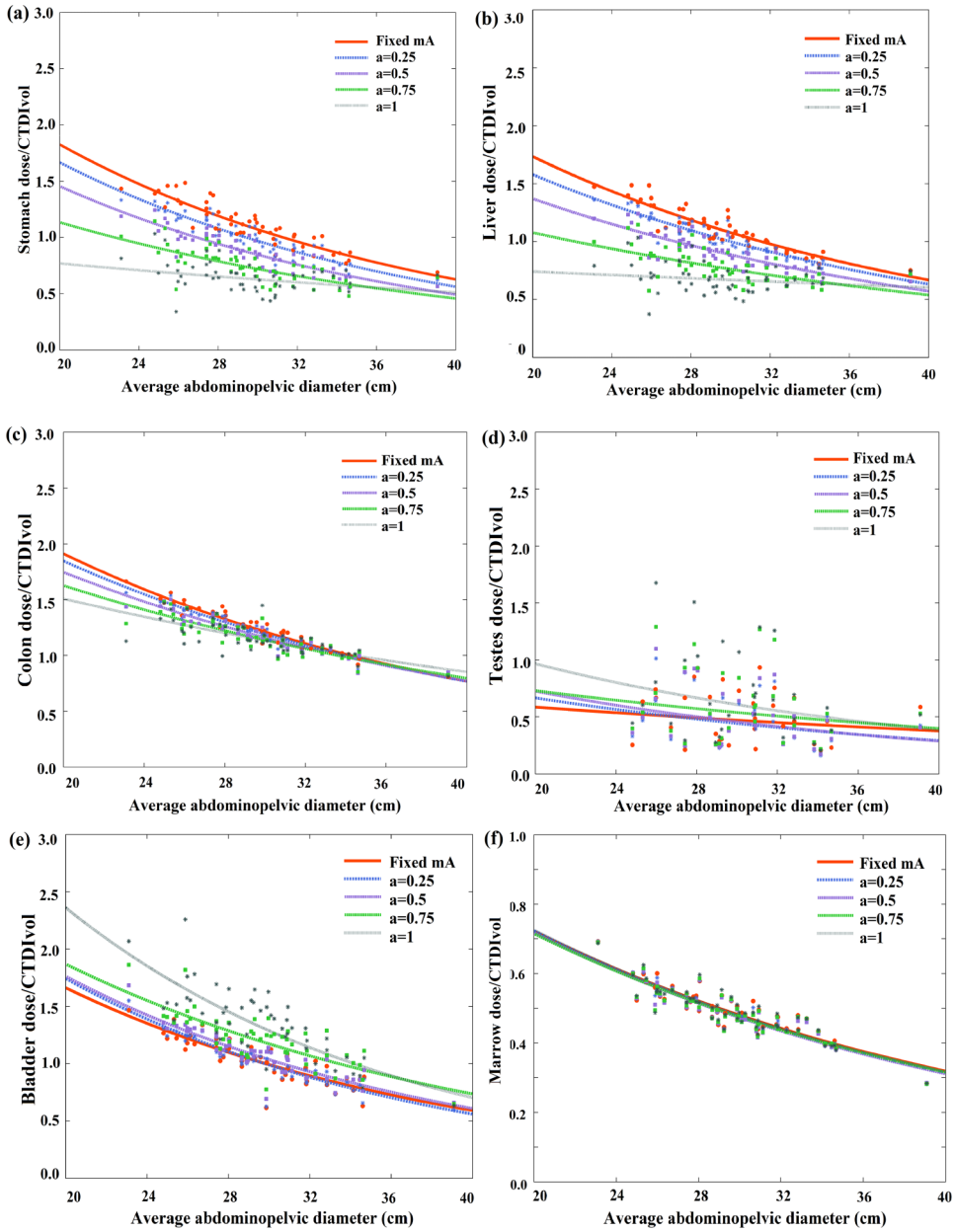

FIG. 5. Example $CTDI_{vol}$-normalized-organ dose coefficients for abdominopelvic scans plotted against the average abdominopelvic diameter at five modulation strengths. Among the five curves, the $CTDI_{vol}$-normalized-organ dose at fixed mA condition ($a = 0$) was used as the prediction basis. The other four curves were used as the gold standard for the prediction.

scan range, if the organ is mismatched, the dose field we applied for the organ [quantified by $(CTDI_{vol})_{organ,weighted}$] can be different from the actual dose field. However, such organ mismatch error is less prominent for distributed organs and organs outside the scan range.

4. DISCUSSION

The governing principle for dose optimization is to determine the minimum amount of radiation dose that achieves the targeted image quality. The fundamental step to achieve that is to prospectively quantify the radiation dose and image quality so that the optimization can be performed prior to the exam in order to minimize individual radiation burden. Within this study, we proposed prediction models for organ dose for clinical chest and abdominopelvic CT exams. The prior information for prediction includes patient anatomical information (trunk height and chest/abdominopelvic diameter), the $CTDI_{vol}$ for the exam, and the tube current modulation profile. The prediction was achieved by combining a patient matching technique and a library of organ dose coefficients from Monte Carlo simulation. Such prediction allows one to potentially optimize the CT protocol by dynamically adjusting the scanning parameters in advance of a CT exam in order to achieve a target diagnostic performance.

As an example of how the prediction models proposed in this study can be implemented for a clinical patient, a 31-

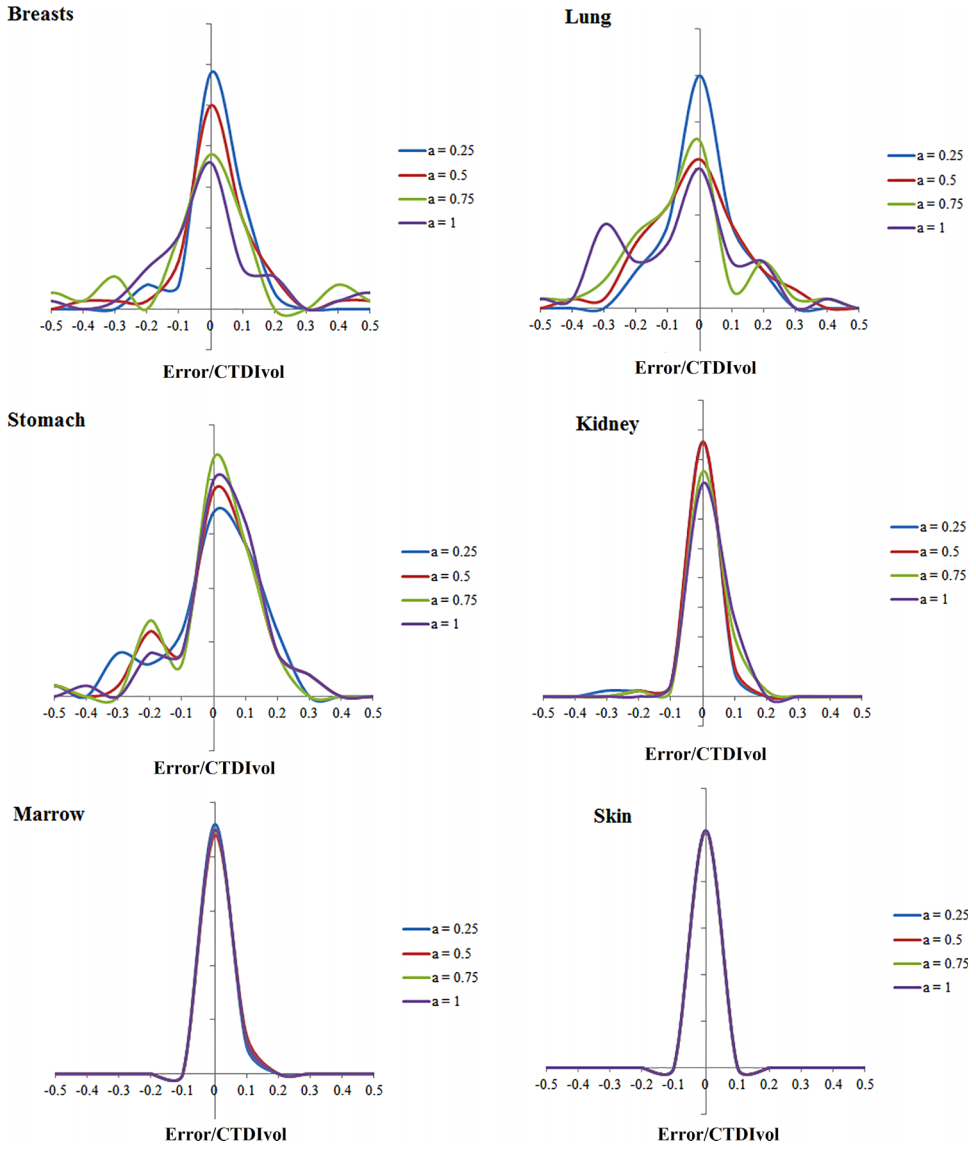

FIG. 6. Histogram of error in predicting organ dose for chest scans. The x axis is determined as the differences between predicted and simulated organ dose normalized by the $CTDI_{vol}$ of the exam.

year-old male patient who undergoes an abdominopelvic CT examination is considered. The $CTDI_{vol}$ for the examination (based on a 32-cm-diameter CTDI phantom) is 7.01 mGy. Given that patients' trunk height is 60.3 cm, one computational phantom in the library was matched to the patient (age 35, trunk height 60.1). Using the h factor estimated based on patient size and the TCM profile of the patient (TCM modulation strength $a = 0.5$), the organ doses were predicted for the patient. The predicted organ doses were compared with the Monte Carlo simulated organ doses with the TCM profile modeled. As shown in Fig. 8, the predicted organ doses agreed well with the expected organ doses.

Several studies have reported the estimation of organ dose under tube current modulation. Schlattl *et al.* proposed organ dose coefficients under tube current modulation for four computational phantoms.[20] The effects of axial and longitudinal TCM modulation were reported. The impact of body stature on dose conversion coefficients was also comprehensively studied. To compare our results against Schlattl *et al.*, three phantoms in Schlattl *et al.* (RCP-AM, RCP-AF, Donna) were matched to phantoms in the XCAT library based on patient height and weight information. The comparison was made for chest scans (TCM modulation strength $a = 0.5$). The differences in TCM organ dose coefficients between the two studies were in the range of 2%–63% across different organs. This difference may be explained by the discrepancies in TCM profiles and adipose composition of the phantoms. Khatonabadi *et al.* studied the organ dose for 32 chest and 39 abdominopelvic exams for a clinical CT system (Sensation 64, Siemens Healthcare, Forchheim, Germany).[12] The study developed an organ-specific $CTDI_{vol}$ to effectively account for the local radiation field under tube current modulation. Li *et al.* estimated organ dose for chest and abdominopelvic scans for a XCAT phantom under five modulation strengths.[1] The study derived a weighted organ-specific $CTDI_{vol}$, which included not only the effect of local mAs variation but

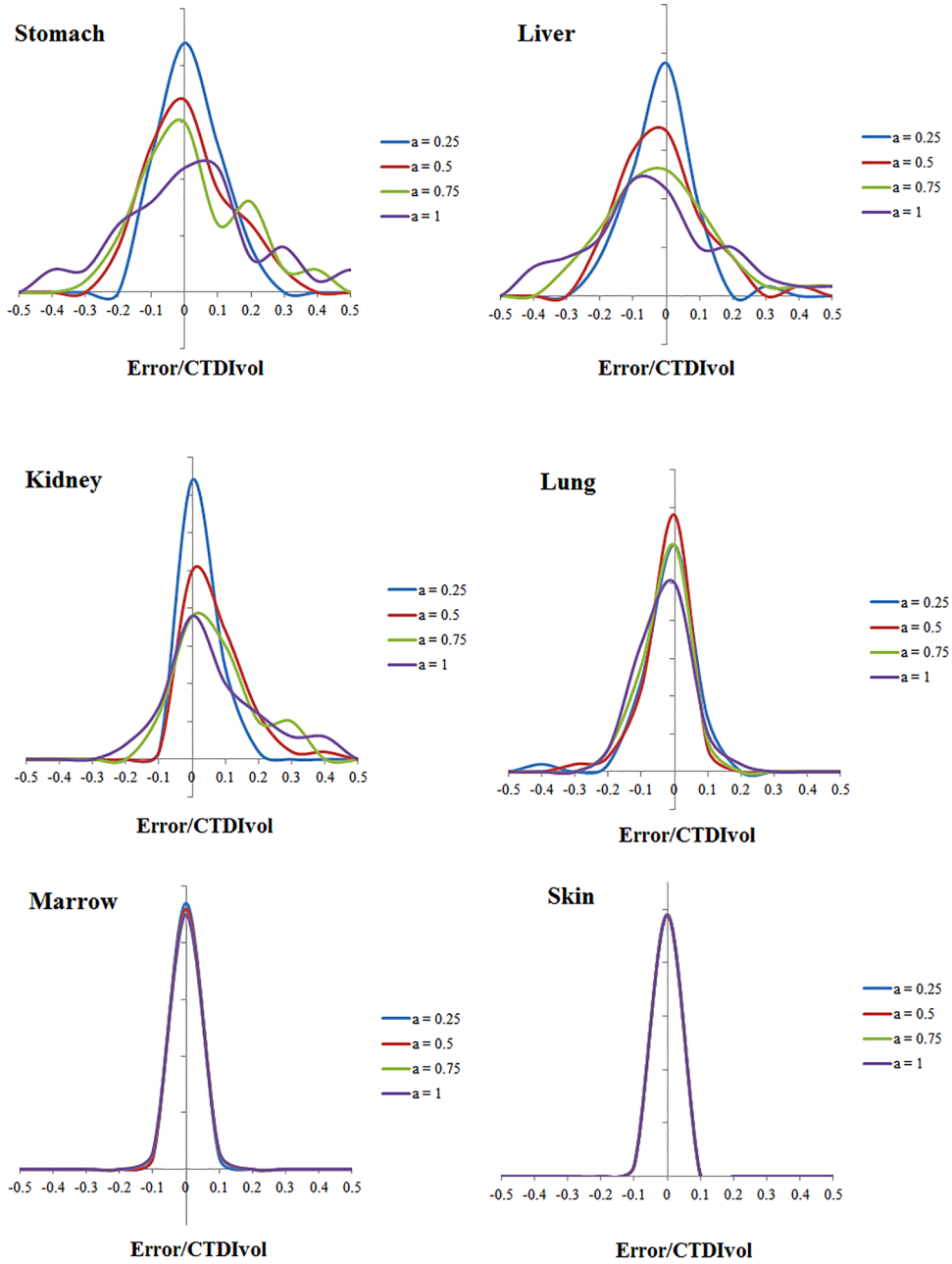

FIG. 7. Histogram of error in predicting organ dose for abdominopelvic scans. The x axis is determined as the differences between predicted and simulated organ dose normalized by the $CTDI_{vol}$ of the exam.

also the variation of organ volume along the z dimension. These prior studies mostly focused on retrospective estimation of organ dose. Our study used a methodology consistent with the previous work to prospectively approximate the local radiation field using weighted $CTDI_{vol}$ values. By using an atlas-based patient matching strategy, our study enables one to predict the organ dose across a large library of patient models at multiple modulation strengths. Such prospective estimation can aid in the design of individualized protocols in relation to a targeted level of image quality.

In this study, we took an empirical approach to assess and predict organ doses in advance of a CT examination. While this empirical approach yielded reasonable accuracy, certain elements of CT irradiation conditions are better to be more fully integrated in this approach. In particular, better accuracy would be expected if the actual dose profile under the TCM irradiation condition was incorporated.[21] This is the topic of continued investigation in our laboratory.

Our study has several limitations. First, we did not explicitly model the tube current modulation profiles to precisely agree with a specific CT system. Furthermore, the TCM profiles generated based on the report from the IMPACT group (published in 2005) may not represent the TCM profiles of more recent CT systems. Further investigation should be conducted in order to model the realistic tube current modulation profiles of the system. Second, the prediction error, while small for the majority of the organs, was relatively

TABLE I. Average differences between organ dose simulated by Monte Carlo (gold standard) and predicted by the patient matching method *for chest scans*. The differences are normalized by the $CTDI_{vol}$ of the exam.

	a = 0.25 (%)	a = 0.5 (%)	a = 0.75 (%)	a = 1 (%)
Kidneys	5.1	4.1	5.5	5.8
Liver	10.6	9.9	9.4	9.6
Gall bladder	8.2	7.8	7.9	8.4
Spleen	17.0	15.8	14.5	14.1
Stomach	14.9	13.8	12.5	12.4
Brain	0.4	0.7	1.0	1.1
Bladder	0.0	0.0	0.0	0.0
Large intestine	2.5	2.4	2.5	2.6
Pancreas	8.9	9.6	10.4	10.8
Prostate	0.0	0.0	0.0	0.0
Adrenals	10.4	10.1	10.1	10.3
Eyes	0.3	0.5	0.7	0.8
Testes	0.0	0.0	0.0	0.0
Small intestine	2.2	2.3	2.6	2.8
Ovaries	0.0	0.0	0.0	0.0
Uterus	0.0	0.0	0.0	0.0
Vagina	0.0	0.0	0.0	0.0
Breasts	6.7	10.1	14.4	16.9
Heart	8.8	8.5	9.4	12.3
Lungs	9.3	12.3	16.0	18.6
Thyroid	23.2	33.2	37.2	39.2
Thymus	13.5	14.4	17.1	21.6
Esophagus	15.7	21.7	26.0	27.3
Bones	4.3	4.3	5.1	5.9
Marrow	3.8	4.4	4.5	4.5
Skin	1.8	1.8	1.8	1.8

TABLE II. Average differences between organ dose simulated by Monte Carlo (gold standard) and predicted by the patient matching method *for abdominopelvic scans*. The differences are normalized by the $CTDI_{vol}$ of the exam.

	a = 0.25 (%)	a = 0.5 (%)	a = 0.75 (%)	a = 1 (%)
Kidneys	3.5	4.6	8.7	11.7
Liver	5.5	6.7	8.8	13.1
Gall bladder	6.6	7.1	7.6	10.5
Spleen	5.8	6.3	6.9	9.3
Stomach	7.6	8.8	9.9	15.1
Brain	0.0	0.0	0.0	0.0
Bladder	13.4	23.2	30.6	33.9
Large intestine	4.3	6.1	7.3	8.1
Pancreas	4.7	5.2	7.3	9.5
Prostate	8.4	15.4	21.9	24.8
Adrenals	4.0	4.4	6.8	9.0
Testes	18.8	19.8	25.0	30.3
Eyes	0.0	0.0	0.0	0.0
Small intestine	5.4	7.0	7.9	8.3
Ovaries	4.5	7.6	12.3	18.2
Uterus	6.7	12.4	15.7	19.8
Vagina	7.8	11.3	16.8	24.8
Breasts	5.9	5.7	5.7	5.8
Heart	9.0	8.3	8.1	8.2
Lungs	4.7	3.8	3.9	4.2
Thyroid	0.7	0.8	0.9	1.1
Thymus	3.2	4.3	5.5	6.4
Esophagus	4.9	4.4	3.9	3.7
Bones	3.6	3.8	4.2	4.9
Marrow	2.4	2.4	2.4	2.4
Skin	1.5	1.5	1.5	1.6

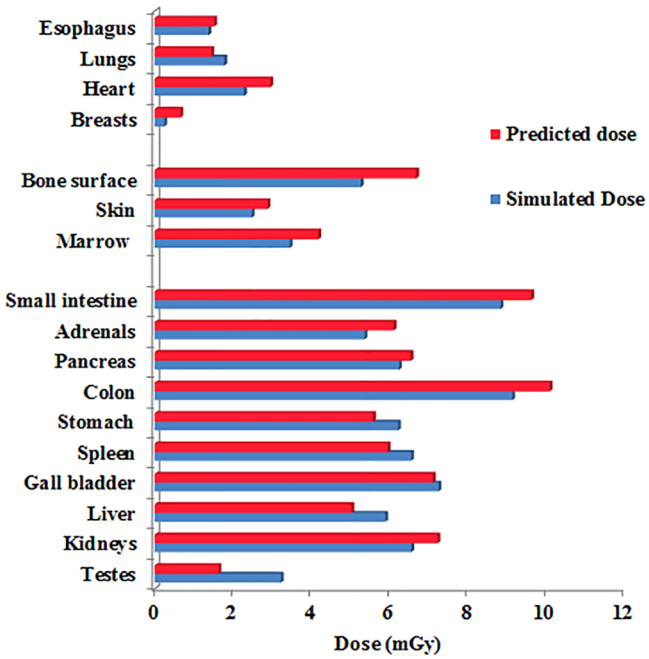

FIG. 8. Predicted and simulated organ dose for a patient (age 31 year old, trunk height 60.3 cm, weight 77.9 kg) undergoing a clinical abdominopelvic protocol.

large for a few organs (thyroid for chest scans; bladder, testes, prostate, ovaries, uterus for abdominopelvic scans). These organs were located centrally in asymmetrical regions of the body. Since the photon flux is highly nonuniform in the x-y plane in these regions, the approximation using fixed-mA coefficients would have limited the accuracy to reflect the dynamic change in the x-y plane. Furthermore, the error induced by patient mismatching may be more prominent for these organs. We are developing correction factors to account for such effects.

5. CONCLUSION

In this study, we developed an atlas-based method to predict organ dose for clinical chest and abdominopelvic exams under tube current modulation. The prediction was achieved by accurately modeling the patient anatomy and the x-ray irradiation field. The predicted organ dose agrees well with the simulate dose with average differences within 1 mGy for both chest and abdominopelvic exams. Such prediction model allows one to optimize the CT protocol by dynamically adjusting the scanning parameters to achieve a

target diagnostic performance with the knowledge of organ dose in advance of a CT exam.

[a]Author to whom correspondence should be addressed. Electronic mail: xt3@duke.edu

[1]X. Li, W. P. Segars, and E. Samei, "The impact on CT dose of the variability in tube current modulation technology: A theoretical investigation," Phys. Med. Biol. **59**, 4525–4548 (2014).
[2]C. H. McCollough, L. Guimaraes, and J. G. Fletcher, "In defense of body CT," AJR, Am. J. Roentgenol. **193**, 28–39 (2009).
[3]D. J. Brenner and E. J. Hall, "Computed tomography–An increasing source of radiation exposure," N. Engl. J. Med. **357**, 2277–2284 (2007).
[4]C. H. McCollough, G. H. Chen, W. Kalender, S. Leng, E. Samei, K. Taguchi, G. Wang, L. Yu, and R. I. Pettigrew, "Achieving routine submillisievert CT scanning: Report from the summit on management of radiation dose in CT," Radiology **264**, 567–580 (2012).
[5]D. P. Frush, L. F. Donnelly, and N. S. Rosen, "Computed tomography and radiation risks: What pediatric health care providers should know," Pediatrics **112**, 951–957 (2003).
[6]D. B. Larson, L. L. Wang, D. J. Podberesky, and M. J. Goske, "System for verifiable CT radiation dose optimization based on image quality. Part I. Optimization model," Radiology **269**, 167–176 (2013).
[7]A. Ding, M. M. Mille, T. Liu, P. F. Caracappa, and X. G. Xu, "Extension of RPI-adult male and female computational phantoms to obese patients and a Monte Carlo study of the effect on CT imaging dose," Phys. Med. Biol. **57**, 2441–2459 (2012).
[8]A. C. Turner, D. Zhang, M. Khatonabadi, M. Zankl, J. J. DeMarco, C. H. Cagnon, D. D. Cody, D. M. Stevens, C. H. McCollough, and M. F. McNitt-Gray, "The feasibility of patient size-corrected, scanner-independent organ dose estimates for abdominal CT exams," Med. Phys. **38**, 820–829 (2011).
[9]X. Tian, X. Li, W. P. Segars, E. K. Paulson, D. P. Frush, and E. Samei, "Pediatric chest and abdominopelvic CT: Organ dose estimation based on 42 patient models," Radiology **270**, 535–547 (2014).
[10]X. Li, E. Samei, W. P. Segars, G. M. Sturgeon, J. G. Colsher, and D. P. Frush, "Patient-specific radiation dose and cancer risk for pediatric chest CT," Radiology **259**, 862–874 (2011).
[11]P. Sahbaee, W. P. Segars, and E. Samei, "Patient-based estimation of organ dose for a population of 58 adult patients across 13 protocol categories," Med. Phys. **41**, 072104 (12pp.) (2014).
[12]M. Khatonabadi, D. Zhang, K. Mathieu, H. J. Kim, P. Lu, D. Cody, J. J. Demarco, C. H. Cagnon, and M. F. McNitt-Gray, "A comparison of methods to estimate organ doses in CT when utilizing approximations to the tube current modulation function," Med. Phys. **39**, 5212–5228 (2012).
[13]W. P. Segars, J. Bond, J. Frush, S. Hon, C. Eckersley, C. H. Williams, J. Feng, D. J. Tward, J. T. Ratnanather, M. I. Miller, D. Frush, and E. Samei, "Population of anatomically variable 4D XCAT adult phantoms for imaging research and optimization," Med. Phys. **40**, 043701 (11pp.) (2013).
[14]W. P. Segars, M. Mahesh, T. J. Beck, E. C. Frey, and B. M. Tsui, "Realistic CT simulation using the 4D XCAT phantom," Med. Phys. **35**, 3800–3808 (2008).
[15]ICRP, "Basic anatomical and physiological data for use in radiological protection: Reference values," ICRP No. 89 (International Commission on Radiological Protection, 2002).
[16]ICRP, "The 2007 recommendations of the international commission on radiological protection," ICRP No. 103 (International Commission on Radiological Protection, 2007).
[17]J. Sempau, J. Baro, J. M. Fernandezvarea, and F. Salvat, "Penelope - An algorithm for Monte Carlo simulation of the penetration and energy-loss of electrons and positrons in matter," Nucl. Instrum. Methods Phys. Res., Sect. B **100**, 31–46 (1995).
[18]J. M. Fernandez-Varea, J. Sempau, E. Acosta, and F. Salvat, "Experimental benchmarks of the Monte Carlo code PENELOPE," Nucl. Instrum. Methods Phys. Res., Sect. B **207**, 107–123 (2003).
[19]N. Keat, Report 05016 CT scanner automatic exposure control systems, London, England, ImPACT, http://www.impactscan.org/reports/Report05016.htm, accessed January 2014.
[20]H. Schlattl, M. Zankl, J. Becker, and C. Hoeschen, "Dose conversion coefficients for CT examinations of adults with automatic tube current modulation," Phys. Med. Biol. **55**, 6243–6261 (2010).
[21]R. L. Dixon and J. M. Boone, "Dose equations for tube current modulation in CT scanning and the interpretation of the associated CTDIvol," Med. Phys. **40**, 111920 (14pp.) (2013).